Acta Biomaterialia 9 (2013) 6834–6843

Contents lists available at SciVerse ScienceDirect

Acta Biomaterialia

journal homepage: www.elsevier.com/locate/actabiomat

Heparin crosslinked chitosan microspheres for the delivery of neural stem cells and growth factors for central nervous system repair

Nolan B. Skop [a,c], Frances Calderon [a], Steven W. Levison [a], Chirag D. Gandhi [b], Cheul H. Cho [c,*]

[a] Department of Neurology & Neurosciences, University of Medicine and Dentistry of New Jersey, New Jersey Medical School, Newark, NJ 07102, USA
[b] Department of Neurological Surgery, University of Medicine and Dentistry of New Jersey, New Jersey Medical School, Newark, NJ 07102, USA
[c] Department of Biomedical Engineering, New Jersey Institute of Technology, Newark, NJ 07102, USA

ARTICLE INFO

Article history:
Received 6 October 2012
Received in revised form 25 February 2013
Accepted 26 February 2013
Available online 5 March 2013

Keywords:
Nerve tissue regeneration
Regenerative medicine
Multifunctional scaffold
Fibroblast growth factor-2
Cell transplantation

ABSTRACT

An effective paradigm for transplanting large numbers of neural stem cells after central nervous system (CNS) injury has yet to be established. Biomaterial scaffolds have shown promise in cell transplantation and in regenerative medicine, but improved scaffolds are needed. In this study we designed and optimized multifunctional and biocompatible chitosan-based films and microspheres for the delivery of neural stem cells and growth factors for CNS injuries. The chitosan microspheres were fabricated by coaxial airflow techniques, with the sphere size controlled by varying the syringe needle gauge and the airflow rate. When applying a coaxial airflow at 30 standard cubic feet per hour, ~300 μm diameter spheres were reproducibly generated that were physically stable yet susceptible to enzymatic degradation. Heparin was covalently crosslinked to the chitosan scaffolds using genipin, which bound fibroblast growth factor-2 (FGF-2) with high affinity while retaining its biological activity. At 1 μg ml^{-1} approximately 80% of the FGF-2 bound to the scaffold. A neural stem cell line, GFP + RG3.6 derived from embryonic rat cortex, was used to evaluate cytocompatibility, attachment and survival on the crosslinked chitosan–heparin complex surfaces. The MTT assay and microscopic analysis revealed that the scaffold containing tethered FGF-2 was superior in sustaining survival and growth of neural stem cells compared to standard culture conditions. Altogether, our results demonstrate that this multifunctional scaffold possesses good cytocompatibility and can be used as a growth factor delivery vehicle while supporting neural stem cell attachment and survival.

1. Introduction

The brain is arguably the most difficult organ to repair after an injury due to the complexity of the central nervous system (CNS) and its limited capacity to regenerate on its own. Neurons do not undergo mitosis and endogenous neural stem cells are unable to replace the quantity of neurons lost after a typical injury. One week post-injury a glial scar forms, which creates an inhibitory environment eliminating the possibility of axonal regeneration [1–3]. Exogenous neural stem cell transplants for brain injury have garnered interest, but effective paradigms for transplanting these cells have yet to be established. Injecting neural precursors directly into the penumbra of an injury has yielded limited success. For example Harting et al. [4] showed that less than 2% of the donor cells engraft and survive in the host brain for 1 year. Transplantation of cells alone may not be enough to overcome the harsh environment, loss of supportive matrix and other problems resulting from brain injury. It follows logically that these cells will benefit from transplantation upon a scaffold [5–8]. One possible reason that the survival rate of transplanted cells is low is that the cystic cavity formed by the injury creates a harsh, non-permissive environment that lacks nutrients, survival factors and, most importantly, a habitable substrate. A scaffold would serve as a structural and functional support for the cells.

Brain injuries are not uniform in shape or size; therefore a scaffold that is injectable and will mold to the injured tissue will be necessary. Hydrogels would fit this criteria; however, cells, particularly neurons, do not extend their processes or neurites efficiently through three-dimensional (3-D) matrices [9–14]. The neurite outgrowth is best observed on 2-D rigid structures. Microspheres contain such a 2-D rigid structure on their surface, as opposed to the 3-D soft structure of hydrogels. Growth cones of neurons pull on their neurites, requiring tension to maintain or initiate neurite extension, which is greater on microspheres than on hydrogels. Another disadvantage using hydrogels is that their biodegradation is hard to control [15,16]. In addition, microspheres can also be fabricated to deliver specific growth and trophic factors to aid cellular engraftment and survival of the transplanted stem cells [17].

* Corresponding author. Tel.: +1 973 596 5381; fax: +1 973 596 5222.
E-mail address: cho@njit.edu (C.H. Cho).

1742-7061/$ - see front matter © 2013 Acta Materialia Inc. Published by Elsevier Ltd. All rights reserved.
http://dx.doi.org/10.1016/j.actbio.2013.02.043

Many biomaterials have been explored in neural tissue engineering applications, including natural materials such as alginate, collagen and Matrigel, or synthetic polymers such as poly(lactic acid) and poly(glycolic acid). Synthetic polymers, while versatile and amenable to adjusting their mechanical or degradation properties, may be inappropriate for brain tissue engineering applications. Firstly, they can leach cytotoxic substances, and, when degraded, their by-products are often acidic, adversely affecting the local brain tissue and increasing inflammation [18]. Furthermore, these polymers are not similar to natural proteins within the body. In particular, they lack the functional groups that natural polysaccharides contain. This results in a lack of cell recognition signals, decreasing the potential for cell adhesion (if desired) and increasing the likelihood that a fibrous scar will form around the scaffold. Natural polymers mimic the native ECM proteins, thus favoring cell interaction or immobilization. However, because these materials are naturally derived, they can be expensive, not readily available and impractical for large scale processing. Another problem may be their immunogenicity, as they are extracted from other animals or plants. Collagen is a common polymer explored in tissue engineering applications that requires some processing to acquire. Although collagen type IV is typically found in the brain, collagen type I is more widely used because it is less expensive. A disadvantage with collagen use in the brain is its potential for foreign body reaction [19]. Matrigel is non-homogeneous protein matrix derived from tumor cells. While cells may interact favorably with this material, it is not a clinically applicable material due to its undefined nature. Other potentially suitable materials, such as hyaluronic acid and fibronectin, are very costly and are difficult to chemically modify.

Chitin is the second most abundant natural polysaccharide in the world next to cellulose. Chitosan is derived by alkaline deacetylation of chitin, which yields repeating units of glucosamine and N-acetylglucosamine in its polymer chains. The percent deacetylation of chitosan governs its properties. The number of acetyl or amine groups at the C2 position determines its mechanical properties, degradation and biocompatibility. Degradation can be easily reduced by crosslinking the polymer. Slowing the degradation time of the scaffold for in vivo applications would enable the biodegradation rate to parallel the rate of new tissue formation [20,21]. Unlike many other polymers, chitosan requires mild processing conditions, dissolving in water with a low acidity (pH < 6.3). Chitosan elicits a minimum foreign body reaction, having been used as an anti-microbial agent [22] and for drug delivery [23], wound healing [20,24] and tissue engineering [25–28]. The US Food and Drug Administration has approved its use in multiple applications. Chitosan has also shown potential in neural tissue engineering applications [7,8,29–33]. Several groups have explored the potential of chitosan as a microcarrier for immunosuppressants [34,35], cancer drugs [36–38] and growth factors [8,29,39]. Guo et al. [40] showed an increase in stem cell survival when transplanted within a chitosan matrix containing Nogo-66 receptor protein in spinal cord injuries.

The cationic nature of chitosan allows interaction with anionic glycosaminoglycans (GAGs) such as hyaluronan or heparin. Heparin is a well-known anticoagulant and plays a role in angiogenesis [41,42], which could aid in revascularizing the damaged cortex. Heparin also has been demonstrated to reduce inflammation [43,44]; thus it may be able to decrease inflammation in the brain and promote engraftment. Another important property of heparin is its high affinity for growth factors such as fibroblast growth factors, hepatocyte growth factor (HGF), platelet-derived growth factor, vascular endothelial growth factor (VEGF) and bone morphogenic protein-6 (BMP-6) [45]. Heparin binds these growth factors and maintains their stability by preventing their thermal degradation [46]. Fibroblast growth factor-2 (FGF-2) is a known survival factor for many types of stem cells, including neural stem cells. During development, FGF-2 promotes neural stem cell self-renewal and maintains the stem cells in a primitive state. It has also been shown to increase the proliferation of the endogenous neural precursors in the subventricular zone following traumatic brain injury, as well as providing neurogenic effects [47,48]. FGF-2 also increases neural stem cell migration and neuronal differentiation [49,50]. Importantly, it binds with high affinity to heparin. The stability and controlled release of FGF-2 over a designated timeframe will help keep the neural stem cells primitive, surviving and proliferating after transplantation.

One of the advantages of using chitosan as the bulk material for a fabricated scaffold is its similarity to natural GAG, which allows easy modification of its side chain groups. Heparin is a naturally occurring highly sulfated GAG that can bind ionically to the amine groups on chitosan via its sulfate and carboxylate side chains. These growth factor–heparin–chitosan complexes can be exploited to produce a biocompatible drug delivery mechanism. Temperature, pH, ions, fluid flow and cytokines may all play a role in the removal of ionically bound heparin as well as degradation of these complexes. Genipin, a plant-derived crosslinking agent, possesses similar mechanical crosslinking properties to the chemical glutaraldehyde, but without its corrosive, cytotoxic and carcinogenic side effects. Mi et al. [51] transplanted chitosan-only microspheres and those crosslinked with glutaraldeyhyde or genipin into skeletal muscles. The genipin crosslinked microspheres elicited less inflammation than the glutaraldehyde crosslinked chitosan. Genipin has been used to covalently bind heparin to chitosan to produce a stable scaffold complex that is ideal for clinical use [52,53]. Genipin has also been suggested to be neurogenic and anti-inflammatory [54–58].

Although chitosan-based microspheres have been widely used in drug delivery and tissue engineering applications, there have been no reports of genipin crosslinked chitosan–heparin complex microspheres for the delivery of neural stem cells and growth factors for CNS repair. In this study, we designed and optimized chitosan-based microspheres as a cellular and growth factor delivery vehicle for nervous tissue regenerative applications. The studies that we performed were designed to test the hypothesis that chitosan–heparin complexes can be used as an effective scaffold for FGF-2 binding and neural stem cell growth and survival.

2. Materials and methods

2.1. Reagents

Chitosan (low molecular weight, ~50 kDa, 75–85% deacetylation), heparin sodium salt from bovine intestinal mucosa and MTT (3-[4,5-dimetylthiazol-2-yl]-2,5-diphenyltetrazolium) were purchased from Sigma (St Louis, MO). Genipin was purchased from Wako Pure Chemical Industries, Ltd. (Osaka, Japan). Lysozyme was purchased from MP Biomedicals (Solon, OH). rh-FGF-2 and FGF-2 enzyme-linked immunosorbent assay (ELISA) kits were purchased from Peprotech (Rocky Hill, NJ).

2.2. Preparation of chitosan microspheres

Chitosan powder (0.5, 1.0, 1.5, 2.0 or 2.5 g) was dispersed in 50 ml of water containing 2.0 vol.% acetic acid to create 1, 2, 3, 4 and 5% chitosan solutions. The chitosan solution was mechanically stirred at 700 rpm until completely dissolved. The resulting solution was collected and centrifuged at 2000 rpm for 10 min. Subsequently, the supernatant was collected and the remaining impurities that pelleted were discarded. Chitosan microspheres were formed using a coaxial airflow technique [59]. Briefly, the

chitosan solution was fed and passed through a syringe with needle gauge of 22G or 30G and with or without different coaxial air pressures using Air Flowmeter (Dwyer Instruments, Inc, Michigan City, IN) (Fig. 1A). The coaxial air applied was: no air = 0, low air = 7, medium air = 12.5, high air = 20 and ultrahigh air = 30 standard cubic feet per hour (SCFH). The spheres were added dropwise to an ionic coagulation bath consisting of 1 M sodium hydroxide:methanol:water (20:30:50 by vol.). The bath was mechanically stirred to prevent spheres from clumping or flattening on the bottom. Next, the spheres were removed from the ionic solution and rinsed four times in distilled water to eliminate any residual sodium hydroxide and methanol.

2.3. BSA release from chitosan microspheres

Genipin-crosslinked and non-crosslinked microspheres were prepared. Prior to sphere formation, 1 mg ml^{-1} of bovine serum albumin (BSA) was dissolved in 3% chitosan solution. The solution was passed through a 30G syringe needle with a coaxial air pressure of 20 SCFH. The chitosan microspheres containing BSA were dispersed in a buffer solution of 50 mM HEPES and 0.9% NaCl (=HEPES buffer solution, HBS) containing 4.50, 0.45 or 0.045 mM genipin and placed on a shaker for 4 h. After crosslinking, the microspheres were rinsed three times with HBS, transferred to a conical tube and resuspended in 2 ml of phosphate-buffered saline (PBS; pH 7.4). The tubes were then placed in a 37 °C water bath. Chitosan microspheres that were not crosslinked with genipin were resuspended in PBS and placed in the water bath immediately after sphere formation. At specific time intervals the supernatant containing the released BSA was removed and stored at −20 °C in Eppendorf tubes. The microspheres that settled at the bottom of the tube were resuspended in fresh PBS after each collection time point. After the last time point, samples were analyzed for protein concentration using the BCA Assay (Thermo Fisher Scientific, Asheville, NC). Absorbance was measured using a microplate spectrophotometer (Molecular Devices, Sunnyvale, CA).

2.4. In vitro degradation studies using lysozyme

Non-crosslinked and crosslinked (0.45 mM genipin) chitosan microspheres were dispersed in 35 mm Petri dishes containing either 2 ml of PBS or 2 ml of 8 mg ml^{-1} lysozyme in PBS. Petri dishes were placed in a 37 °C incubator, to simulate physiological temperatures, for several days. One milliliter of the PBS or lysozyme solution was replaced every 3 days. Spheres were rinsed with PBS and serially dehydrated in ethanol. Next they were air dried overnight and vacuum dried for 4 h prior to scanning electron microscopy (SEM) analysis.

2.5. Swelling and stability test

The swelling and stability of microspheres were determined by examining morphological and size changes after dehydration and hydration in PBS. Non-crosslinked and crosslinked (0.45 mM genipin) chitosan microspheres were formed using the technique described above. They were either dehydrated overnight or seeded directly in 300 μl of PBS in a 96-well plate. The plate was placed in the 37 °C incubator for several days and 100 μl of PBS was replaced every 3 days. Optical images of microspheres were captured over a given period of time and microsphere diameters were measured. Dehydrated sphere diameters were compared upon rehydration in PBS and analyzed using Sigma Scan Pro 5 software.

2.6. Ionic and covalent heparin immobilization on chitosan films and microspheres

Two-dimensional chitosan films and 3-D chitosan microspheres were prepared for ionic and covalent heparin immobilization. To prepare the chitosan films, 24-well plates were coated with a thin layer of 3% chitosan solution. The wells were allowed to dry overnight and subsequently the acidity was neutralized using 0.5 M sodium hydroxide. Afterwards, plates were rinsed three times with distilled water and incubated overnight with 0.5 mg ml^{-1} heparin in HBS for ionic binding and in 0.45 mM genipin in HBS for covalent binding. The next day, solutions were aspirated from each well and rinsed three times with HBS. To characterize and compare ionic and covalent immobilization of heparin on the chitosan surfaces, half of the coated wells from each condition were incubated in 1.5 M NaCl for 30 min on an orbital shaker at room temperature to remove ionic heparin binding. The remaining wells were incubated in HBS for comparison. Immobilized heparin was detected by the toluidine blue dye. Briefly, a solution of 3 mg ml^{-1}

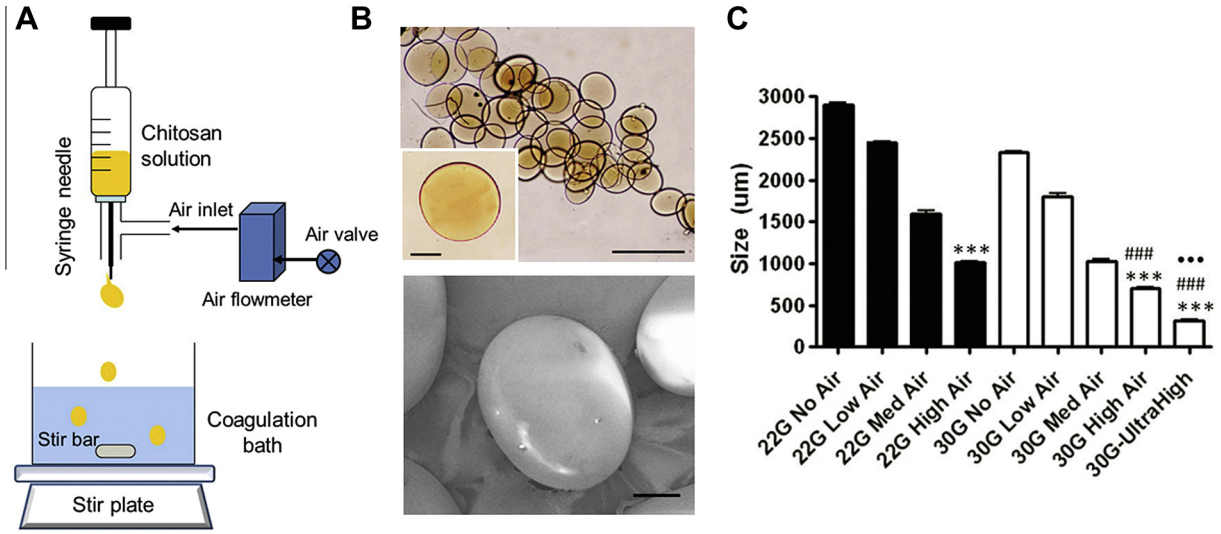

Fig. 1. Fabrication of chitosan microspheres. (A) Schematic of the formation of chitosan microspheres using a coaxial airflow generator. (B) Morphology of microspheres by phase contrast microscopy (top) and SEM (bottom). (C) Effect of airflow rate and syringe needle gauge size on the microsphere size. Values represent mean ± SE (n = 25). Statistical significance was determined by one-way ANOVA using Tukey's post hoc test. $^{***}p < 0.001$ vs. 22G No Air and 30G No Air, $^{###}p < 0.001$ vs. 22G High Air. $^{•••}p < 0.001$ vs. 30G High Air. Scale bars: (B) 1000 μm, inset = 200 μm (top), 100 μm (bottom).

toluidine blue was added to each well. After 10 min, toluidine blue was removed by aspiration and wells were washed gently twice with HBS. Images were acquired with a digital color camera (Nikon DS-Ril) and an inverted fluorescence microscope (Nikon Ti-S). For 3-D chitosan heparin immobilization, microspheres were prepared as described above and treated as described for 2-D films.

2.7. Fourier transform infrared spectroscopic analysis

The genipin crosslinked chitosan–heparin films were analyzed with attenuated total reflectance Fourier transform infrared spectroscopy (ATR-FTIR; Perkin Elmer) to detect heparin binding. As controls, the chitosan film and heparin powder were measured by FTIR.

2.8. Scanning electron microscopy

Samples were fixed with 2.5% glutaraldehyde in PBS for 24 h at 4 °C. After fixation, the samples were washed three times with PBS, dehydrated through an ethanol series and then vacuum dried. The dried samples were coated with carbon and imaged by SEM (LEO 1530 FE-SEM, Carl Zeiss Microscopy).

2.9. Growth factor binding to heparin

The levels of FGF-2 immobilized by chitosan–heparin complexes were evaluated by ELISA. Two-dimensional chitosan films were prepared as described above in 96-well plates using 50 μl per well of 3% chitosan. Chitosan coated wells were incubated overnight with HBS only or HBS containing 0.45 mM genipin or 0.5 mg ml^{-1} heparin, or both genipin and heparin. The following day, the wells were aspirated, rinsed three times with fresh HBS and incubated for 3 h at room temperature with 100 μl of increasing concentrations of FGF-2 (100, 500, 1,000 ng ml^{-1}) or no growth factor. The FGF solutions contained 1 mg ml^{-1} BSA to maintain growth factor stability. After allowing the FGF-2 to bind, the solutions were collected in separate Eppendorf tubes to determine the unbound FGF-2. Each well was washed gently twice with 50 μl of HBS, which was also added to each respective collection tube. To test long-term release, wells were refilled with 100 μl of PBS and collected 7 days later. A sandwich ELISA was used to measure the FGF-2 that was released over time. Subtracting the amount released on day 0 from the total amount of FGF-2 added to the scaffold revealed the percentage of growth factor bound.

2.10. RG3.6 neural stem cell culture

GFP$^+$ RG3.6 cells are a neural stem cell line derived from embryonic day 13.5 rat cortex (generous gift from Dr. Martin Grumet, Rutgers University, New Brunswick, NJ). Cells were maintained in DMEM/F12 medium supplemented with B27, gentamycin (50 μg ml^{-1}), apo-transferrin (50 μg ml^{-1}) and daily addition of FGF-2 (10 ng ml^{-1}).

2.11. MTT reduction assay

The MTT assay is a colorimetric assay that measures the reduction of yellow MTT in the cell into insoluble purple formazan [60]. Briefly, 10 μl of a 5 mg ml^{-1} MTT solution in PBS was added to 100 μl of medium and incubated for 4 h in a cell incubator at 37 °C. The reaction was stopped by adding 100 μl of a solution containing 50% (w/v) *N*,*N*-dimethylformamide and 20% SDS (pH 4.8). The plates were maintained overnight in the incubator at 37 °C and the absorption values at 560–690 nm were determined using an automatic microtiter plate reader.

2.12. Biological activity of bound FGF-2

To evaluate the biological activity of bound FGF-2, the survival/proliferation of RG3.6 cells grown on FGF-bound 2-D chitosan films was measured using the MTT assay. FGF-2 (1 μg ml^{-1}) was added to chitosan–heparin–genipin films at 37 °C for 3 days. Subsequently, GFP + RG3.6 cells were seeded at a density of 6.25×10^4 - cells cm^{-2} in 96-well plates in Neurobasal medium supplemented with B27, gentamycin (50 μg ml^{-1}) and apo-transferrin (50 μg ml^{-1}). RG3.6 cells were also seeded into wells with freshly bound FGF-2 (Bound Day 0). A third set of control cells were seeded onto chitosan-only films containing 10 ng ml^{-1} FGF-2 in the medium. A fourth set of cells were seeded on genipin crosslinked chitosan–heparin complex films that lacked bound FGF-2 or FGF-2 in the medium. Each film was coated with 10 μg ml^{-1} fibronectin solution to enhance cell attachment to substrates. Ten percent of the growth medium was changed daily, using Neurobasal medium without FGF-2 for most conditions and Neurobasal medium containing 100 ng ml^{-1} FGF-2 for the control condition only. The MTT assay was performed after 2 days in vitro.

2.13. Study of cell adherence to chitosan microspheres

To test the cytocompatibility of the chitosan microsphere, the RG3.6 cells were cultured on microspheres generated by ionic coagulation with a 30G needle and a 20 SCFH coaxial airflow rate. In order to enhance cell attachment, microspheres were incubated in 10 μg ml^{-1} fibronectin solution overnight prior to cell seeding. RG3.6 cells were seeded at a density of 100,000 cells per well in 24-well plates onto microspheres immersed in medium consisting of DMEM/F12 supplemented with B27, gentamycin (50 μg ml^{-1}), apo-transferrin (50 μg ml^{-1}) and FGF-2 (10 ng ml^{-1}). Cells were fed by replacing 10% of the medium containing 10 times the initial concentration of FGF-2 (100 ng ml^{-1}) every day and 50% of the medium was changed every third day with medium containing 20 ng ml^{-1} FGF-2. The cells were cultured on the microspheres for 7 days. The cultured cells were imaged using optical, fluorescent and scanning electron microscopes.

2.14. Statistical analysis

Data are expressed as the mean ± standard error of mean (SE). Statistical analysis was performed by GraphPad Prism 4 and one-way analysis of variance (ANOVA) using Tukey's post-hoc. Probability values less than 0.05 were considered statistically significant.

3. Results

3.1. Fabrication and characterization of chitosan microspheres

Chitosan microspheres were prepared by ionic coagulation whereby a chitosan solution (acidic) is dropped via a syringe into a basic coagulation bath comprising sodium hydroxide, methanol and deionized water. This is the preferred technique for sphere formation for cell transplantation because others require the use of more caustic chemicals. The percent chitosan used for sphere formation ranged from 1 to 5% w/v. The 1% chitosan solution did not form spheres, whereas the 2% chitosan solution produced deformed structures that were oblong in shape. Microspheres formed using 3% chitosan were spherical in shape with a smooth surface, as observed by phase contrast (Fig. 1B, top) and SEM (Fig. 1B, bottom). The 4% chitosan solution formed structures that were oblong and pinched off at one end due to increased viscosity of solution and increased surface tension at the syringe opening. The 5% chitosan solution was too viscous to pass through the syringe. Micro-

sphere size was determine by the needle gauge used and the coaxial airflow applied (Fig. 1C). Small diameter needles resulted in small microspheres. Further reductions in size could be achieved by increasing the coaxial airflow. High airflow (20 SCFH) with a 30G needle produced microspheres that ranged from 500 to 700 μm in diameter. A subsequent test was performed to determine the maximum coaxial air pressure before failure occurred. Microspheres were created that were approximately 300 μm using a coaxial airflow of ultrahigh airflow (30 SCFH) with a 30G needle, but these structures were not spherical. At pressures above 35 SCFH the chitosan solution splattered and the structures were not spherical.

3.2. Protein release

Towards the goal of producing a scaffold that would release growth and trophic factors, the cumulative release of encapsulated BSA was plotted as a function of time. Fig. 2A depicts the cumulative release of BSA from non-crosslinked microspheres and microspheres crosslinked with 4.5, 0.45 and 0.045 mM genipin. An initial burst release effect was observed during the first hour followed by slow release, which was most prevalent for the non-crosslinked spheres. As the genipin concentration increased, the release of encapsulated BSA was reduced. Using 4.5 mM genipin crosslinked microspheres, the release profile was highly attenuated, releasing approximately 8.5% of the encapsulated BSA within the first 4 h, with an additional release of only 2.7% more over the next 30 days. Non-crosslinked and 0.045 mM genipin crosslinked microspheres expelled most of their encapsulated BSA within the first 24 h, releasing 30 and 25% respectively during that time. Genipin at 0.45 mM showed the most favorable and steady release profile. This concentration allowed for an initial burst effect of 17% and steadily released approximately 1.5–2% BSA every week. Thus, this study demonstrated that chitosan microspheres crosslinked with a specific concentration of genipin could be used as an effective method to slowly deliver a drug or protein. However, a limitation of this technique is that it is inefficient. Most of the encapsulated BSA was lost prior to the start of the study. BSA was not only lost while the microspheres were forming in the coagulation bath but also during the washes used to remove the remaining NaOH and methanol. Over 50% of BSA was lost at this step of the protocol.

3.3. Swelling properties and stability test

As swelling of the scaffold in vivo could cause adverse effects to the surrounding native tissue or increased intracranial pressure resulting in possibly more bystander damage, it was important to determine the stability of the microspheres. Cross-linked and non-crosslinked microspheres both swelled dramatically from a dry state to a wet state. As expected, compared to other conditions, highly crosslinked spheres using 4.5 mM genipin exhibited less swelling, with an increase in sphere diameter to 224.1 ± 4.3% (Fig. 2B). Spheres crosslinked with 0.045 mM genipin swelled more (261.3 ± 2.7% increase in sphere diameter) than others. Since the spheres will already be hydrated prior to cell seeding and transplantation, their swelling/stability properties over time is more important. Microspheres demonstrated very little change in size over time when incubated in PBS. Cross-linked microspheres swelled minimally over time compared to the non-crosslinked spheres (Fig. 2C). Spheres without genipin decreased in size by

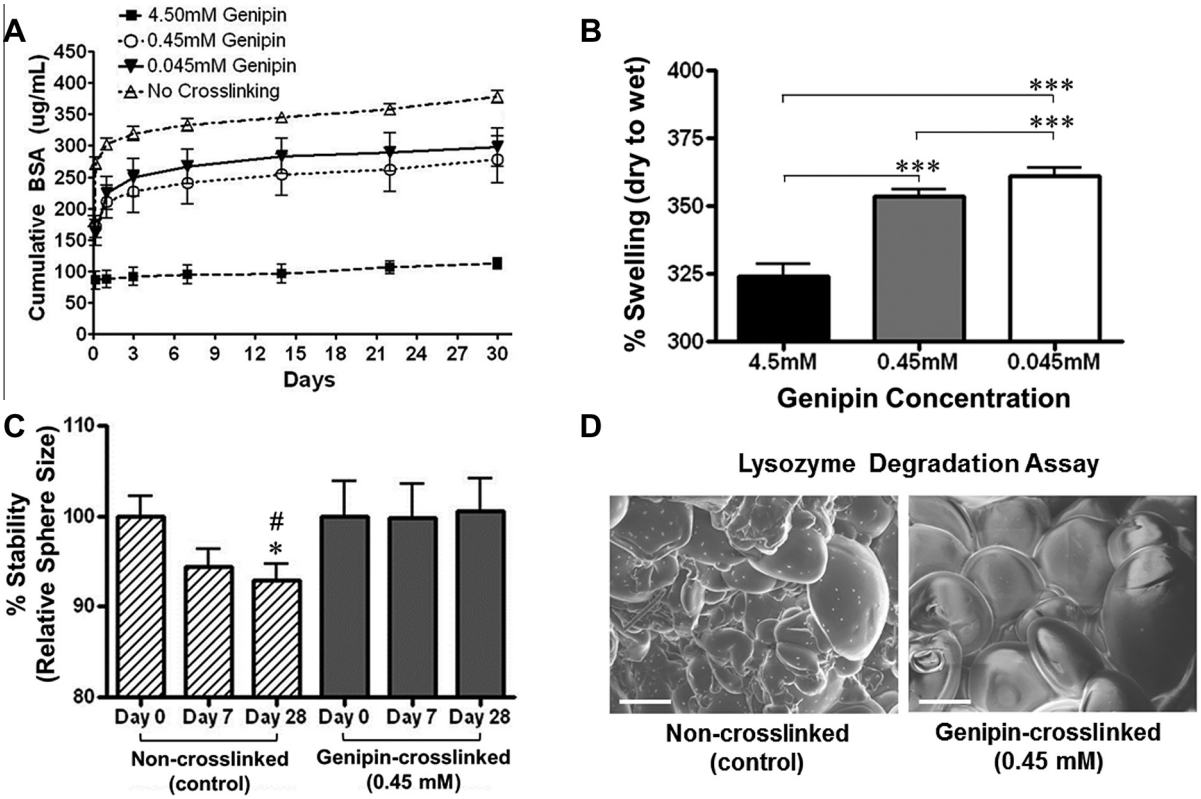

Fig. 2. Effect of crosslinking of chitosan microspheres. (A) Release of BSA that had been incorporated in the chitosan prior to microsphere fabrication. Values represent mean ± SE (n = 3). (B) Measurements of swelling (%, dry to wet) at different concentrations of genipin. The sphere sizes in the wet state were normalized to those in the dry state. Values represent mean ± SE (n = 30). $^{***}p < 0.001$. (C) Measurements of stability (%) of crosslinked and non-crosslinked microspheres. The sphere sizes at each time point were normalized to those at day 0. Values represent mean ± SE (n = 35). $^{*}p < 0.05$ (day 0 vs. day 28). $^{\#}p < 0.05$ (non-crosslinked vs. genipin-crosslinked on day 28). (D) SEM images of microspheres incubated in 8 mg ml^{-1} lysozyme solution for 7 days. Scale bars, 100 μm.

7% over a 1 month period in PBS. This can likely be attributed to a small degree of degradation. Spheres crosslinked using 0.45 mM genipin spheres swelled 0.5% over a period of 1 month in PBS. This percentage change over the month is low enough to not cause significant damage.

3.4. In vitro degradation studies using lysozyme

To model the biodegradability of the microspheres, in vitro studies were performed to evaluate the stability of the microspheres when incubated at 37 °C in either a balanced salt solution or a solution containing 8 mg ml^{-1} lysozyme and evaluated at 7 and 28 days in vitro. Non-crosslinked and chitosan microspheres crosslinked with 0.45 mM genipin were compared. Non-crosslinked spheres showed signs of mild surface erosion after 1 week in PBS (data not shown). By contrast, non-crosslinked microspheres incubated in lysozyme solution mostly lost their spherical structure after 1 week (Fig. 2D, left). At the same time point, crosslinked spheres incubated in lysozyme displayed modest to no degradation (Fig. 2D, right). Non-crosslinked chitosan spheres continued to degrade at a faster rate than the crosslinked microspheres. At 1 month the non-crosslinked samples lost their integrity and were reduced to fragments (data not shown). The crosslinked samples showed signs of degradation by 1 month, but retained much of their original shape. This in vitro test demonstrates that crosslinking the chitosan microspheres reduces the rate at which they can be enzymatically dissolved, thus reducing the amount of swelling in the spheres. Reducing swelling would be beneficial, as swelling increases intracranial pressure, thus contributing to inflammation and causing a greater amount of cell death. However, the caveat is that, with increased crosslinking, the degradation of chitosan microspheres decreases, increasing their durability and half-life in vivo.

3.5. Heparin binding to chitosan

Heparin promotes angiogenesis, has been demonstrated to reduce inflammation and has high affinity for fibroblast growth factors, thus we reasoned that it would be highly advantageous to covalently attach heparin to the microspheres. Fig. 3A shows the chemical structures of chitosan, heparin and genipin. Heparin binding to chitosan was tested in two ways, via colorimetric dye staining and FTIR analyses. Positively charged toluidine blue stain, which stains for negatively charged heparin, was strong on chitosan–heparin 2-D films and 3-D microspheres (Fig. 3B). Toluidine blue also strongly stained the chitosan–heparin–genipin films and microspheres. As expected, the chitosan-only control did not demonstrate any toluidine blue stain on films and microspheres. The blue staining on the rim of the chitosan-only condition is due to the toluidine blue getting trapped underneath the thin edges of the chitosan coating. This was difficult to avoid, thus only the centers of the films were considered for analyses. When the films or microspheres were immersed and washed in 1.5 M NaCl instead of HBS, the chitosan alone remained unstained, as expected. However, when the chitosan–heparin films and microspheres (ionic binding) were washed with NaCl followed by toluidine blue, a small amount of stain was detected. By contrast, the chitosan–heparin–genipin samples (covalent binding) showed the same positive toluidine blue staining after the NaCl wash as with HBS (both 2-D and 3-D). This is because the NaCl wash removed the ionic binding between chitosan and heparin, but did not remove the covalent binding between chitosan and heparin when genipin crosslinker was added. The FTIR results confirmed successful immobilization of heparin on the chitosan by genipin crosslinking (0.45 mM). FTIR spectra of genipin crosslinked chitosan–heparin complex exhibited peaks at 1230 nm and 820 nm, representing S=O and C–O–S stretches of sulfate groups from heparin, respectively (Fig. 3C). The chitosan–heparin complex also displayed peaks of chitosan functional groups, including N–H bending at 1560 nm and CH_2 bending at 1380 nm. These results demonstrate that 0.45 mM was an appropriate concentration of genipin to effectively bind chitosan and heparin. A higher concentration of genipin (4.5 mM) resulted in extensive crosslinking, which eliminated binding sites on the chitosan and heparin; therefore the same sulfate and carboxylate peaks were not seen (data not shown). At the lower concentration of genipin (0.045 mM), insufficient covalent bonds were formed between heparin and chitosan.

3.6. Growth factor immobilization and release

Heparin has binding sites for several growth factors, including but not limited to FGFs, VEGF, HGF and BMP. Therefore we investigated the levels of FGF-2 that could be immobilized by chitosan–heparin complexes. Three different concentrations (100, 500 and 1,000 ng ml^{-1}) of FGF-2 were evaluated for binding to chitosan–heparin–genipin film scaffolds. As predicted, as the concentration of FGF-2 increased, the amount of bound FGF-2 increased (Fig. 4A). At each concentration approximately 70–80% of the FGF-2 bound to the scaffold (Fig. 4B). To evaluate the bioactivity of the immobilized FGF-2, a neural stem cell line, RG3.6, was seeded onto a 2-D chitosan–heparin–genipin-crosslinked scaffold and the MTT assay was performed to assess the cell viability and growth after 2 days in vitro. Cells were tested under four conditions: they were seeded onto (i) the complex film with FGF-2 in the medium (Control); (ii) the complex film with freshly bound FGF-2 (Bound, Day 0); (iii) the complex film where FGF-2 had been bound earlier and incubated at 37 °C for 3 days (Bound Day 3); or (iv) the complex film without added FGF-2 in the medium. Neural stem cell growth and viability as reflected by the MTT assay was highest on the FGF-2 bound to the scaffold immediately prior to cell seeding. Cell growth on the bound FGF-2 condition was superior to cell growth on the scaffold with FGF-2 provided in the medium. Interestingly, cell growth on the complex film that had immobilized FGF-2 attached to the scaffold 3 days prior to seeding was comparable to the control, which received FGF-2 added to the medium daily (Fig. 4C). Cell growth on both of the FGF-2-containing scaffolds as well as the control was significantly greater than the cell growth on the complex film lacking FGF-2 in the medium. When analyzing growth factor release over 1 week (data not shown), a small amount of FGF-2 was detectable through ELISA. However, it is difficult to tell whether the slight decrease in MTT values between the freshly tethered FGF-2 (Day 0) and the FGF-2 bound for 3 days (Day 3) can be attributed to this release or to loss of activity. Phase contrast images of the neural stem cells maintained under these growth conditions paralleled the MTT results (Fig. 4D–G).

3.7. Cell attachment to microspheres

The biocompatibility of a 3-D construct was tested using the neural stem cell line RG3.6. As shown in Fig. 5, the cells attached to the microspheres within 12 h after plating. When attached to the microspheres the RG3.6 cells exhibited a primitive morphology, which was characterized by two or three processes that were quite long. The morphology of these cells resembled typical neural precursors derived from the embryonic ventricular zone, known as radial glia. Radial glia have few, but long, processes that extend to the pial surface of the brain during development. They proliferate to produce neocortical neurons. Most of these cells expressed green fluorescent protein (GFP), thus suggesting a high viability (Fig. 5C). SEM images (Fig. 5D) revealed their spatial structure and the 3-D morphologies of the neural stem cells seeded on the

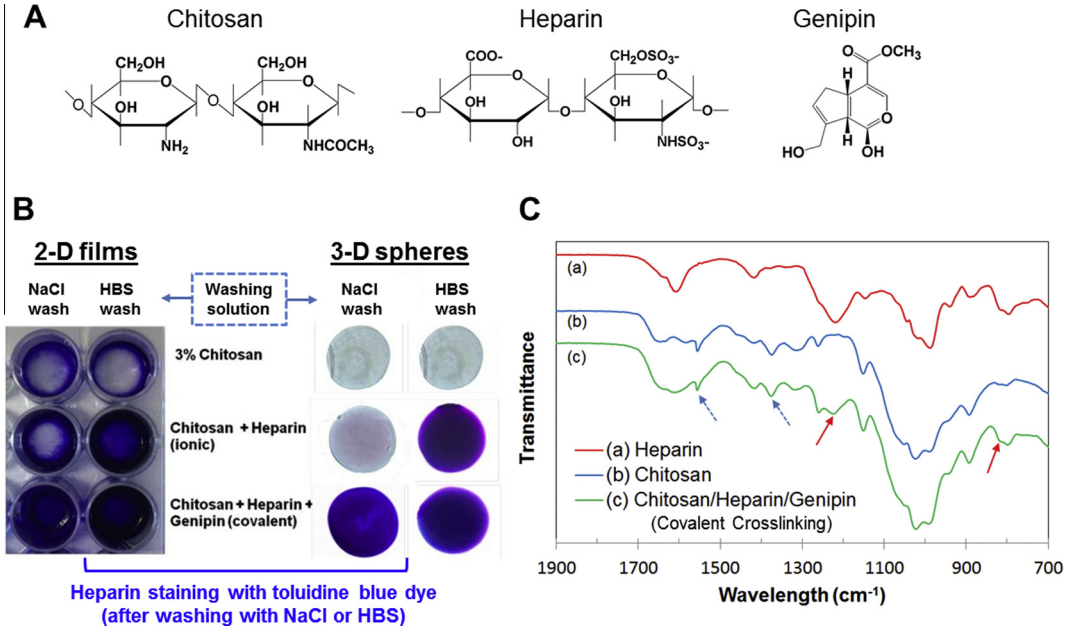

Fig. 3. Ionic and covalent immobilization of heparin on the 2-D chitosan films and 3-D microspheres. (A) Chemical structures of chitosan, heparin and genipin. (B) Heparin bound to 2-D and 3-D substrates was either crosslinked using 0.45 mM genipin or allowed to attach via ionic interactions only. The wells were washed with either HBS or 1.5 M NaCl, and heparin retention was measured by toluidine blue dye staining. (C) FTIR spectra of heparin, chitosan and genipin-crosslinked chitosan–heparin complex. Arrows indicate functional groups for heparin (red) and chitosan (blue) from the genipin-crosslinked chitosan–heparin complex.

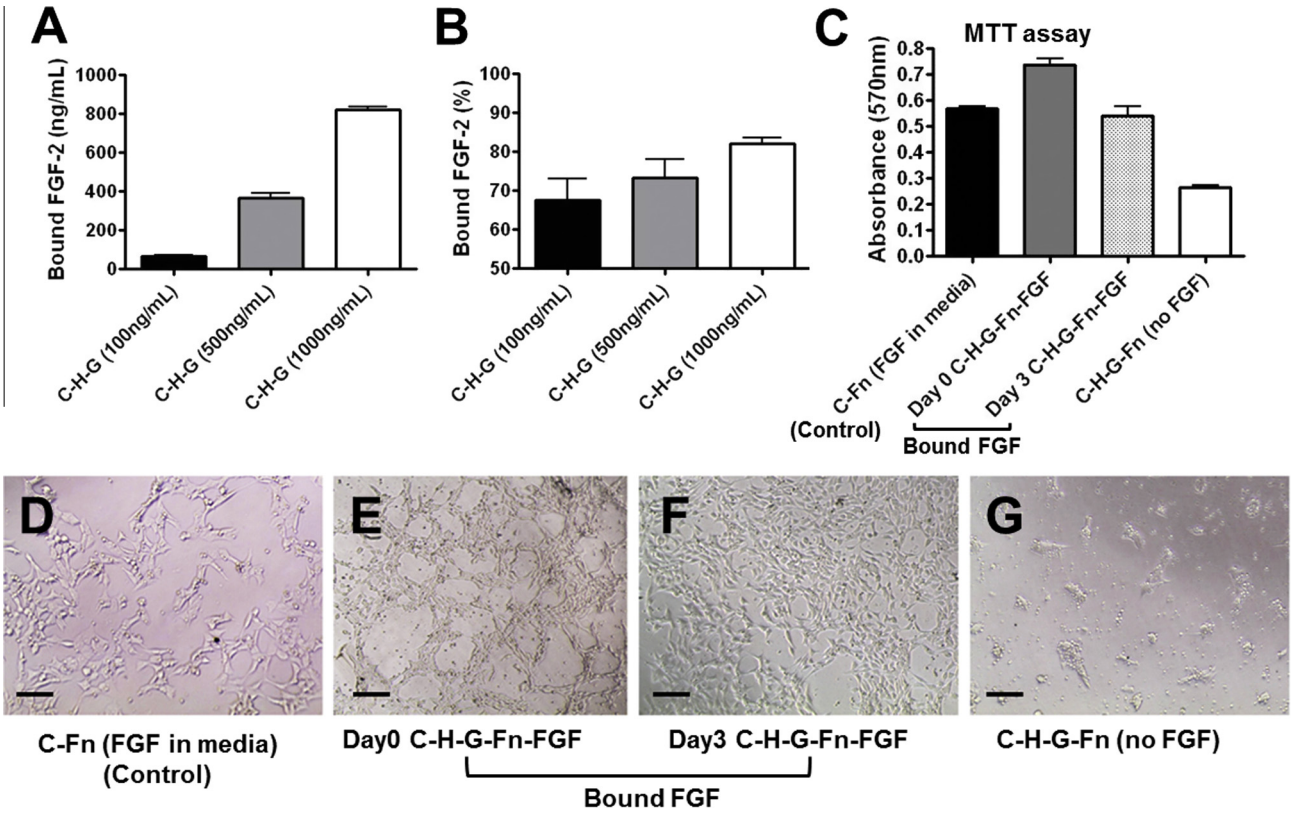

Fig. 4. FGF-2 bound to the genipin-crosslinked chitosan–heparin complex film retains its biological activity. (A) Results of an FGF-2 ELISA to determine the amount of FGF-2 bound to the complex film at different concentrations. (B) Efficiency of FGF-2 binding at different concentrations. (C) Results of an MTT assay to evaluate biological activity. The GFP + RG3.6 neural stem cell line was seeded at a density of 6.25×10^4 cells cm^{-2} in 96-well plates in B27-supplemented Neurobasal medium onto chitosan coated with fibronectin with FGF-2 in the medium (control), the complex film with freshly bound FGF-2 (Bound, Day 0), the complex film where the FGF-2 had been bound 3 days earlier and incubated at 37 °C for 3 days (Bound, Day 3) or the complex film without added FGF-2 in the medium. The MTT assay was performed after 2 days in vitro as an index for the numbers of viable cells. Absorbance at 570 nm was measured and the results are reported after subtracting the background absorbance measured at 690 nm. (D–F) Phase contrast images of the neural stem cells on the various substrates. Scale bars: (D–G) 100 μm. Values represent mean ± SE (n = 3).

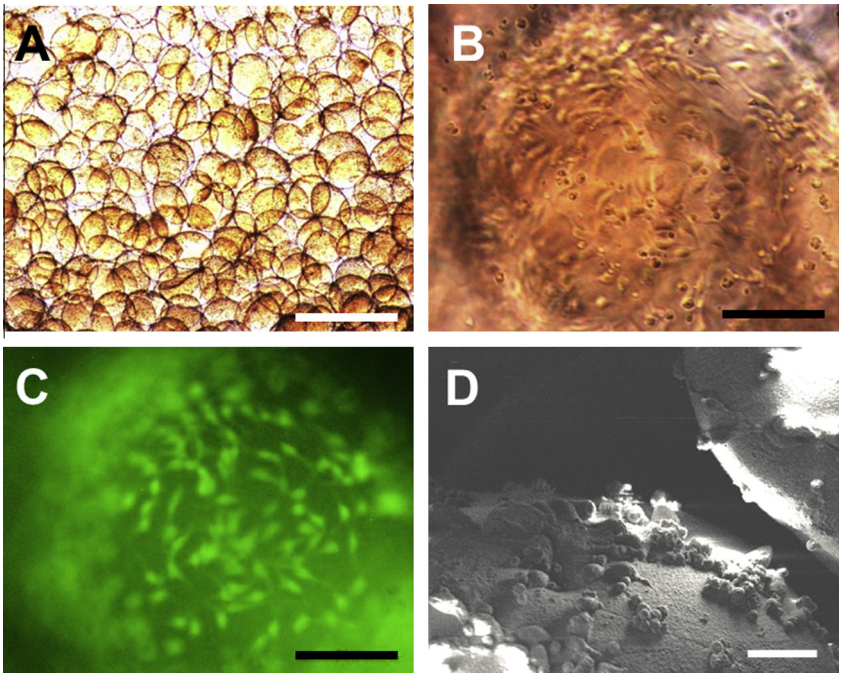

Fig. 5. Morphology of neural stem cells (GFP + RG3.6) cultured for 7 days on the chitosan microspheres. (A) Phase contrast image of microspheres at low magnification. (B) Phase contrast images of the RG3.6 neural stem cells attached to microspheres at higher magnification. (C) GFP + expression of the RG3.6 cells. (D) SEM images of two microspheres with attached the RG3.6 cells. Scale bars: (A) 1000 μm, (B, C) 100 μm, (D) 20 μm.

microspheres for 7 days, which is in accordance with the phase contrast images shown in Fig. 5A and B. The results of this study demonstrate that the neural stem cells attach and spread well on the chitosan-based microsphere scaffolds, indicating good cytocompatibility.

4. Discussion

A primary goal of these studies was to develop a multifunctional scaffold that will serve as a delivery system and structural support for transplanted cells to promote regeneration of the CNS after injury. An effective microsphere scaffold will increase the survival and proliferation of the engrafted cells through its design and release of essential growth and trophic factors. To evaluate the time course of release of an encapsulated growth factor from the microspheres we measured the release of encapsulated BSA using the Bradford assay. These studies show that chitosan microspheres are capable of releasing a desired peptide that can be controlled through chemical crosslinking. This technique of crosslinking naturally occurring biomaterials for protein release has been used by many groups [53,59,61–64]. Yuan et al. (2007) demonstrated similar effects on albumin release from genipin-crosslinked chitosan microspheres. They showed that the amount of protein elution could be controlled by the duration of time the albumin-containing microspheres spent in a fixed concentration of genipin. Similar to this study, the highest percentage of BSA release was seen in the chitosan-only condition, but as a burst effect. Uncrosslinked chitosan is not ideal for transplantation as the rate of degradation might be too fast to promote new tissue ingrowth. The degree of deacetylation (DD) of chitosan plays a large role in governing not only its physiochemical properties but also its degradation. The process of deacetylation involves the removal of acetyl groups from the molecular chain of chitin, resulting in the formation of chitosan. This compound possesses a high degree of chemically reactive amino groups ($-NH_2$) [34]. The more it is deacetylated, the greater the number of free amine groups, which allows for side chain modification. Additionally, an increase in free amine groups enables more crosslinking between chitosan polymer chains. With a higher crosslinking density, the swelling and degradation of the material can be reduced [65]. Degradation of chitosan is inversely proportional to the DD because high DD materials also tend to have more hydrogen bonding and crystallinity, which limits enzymatic attack and helps stabilize molecules as compared with low DD materials [20,66,67].

The higher the deacetlyation, the less inflammatory response and the slower it is degraded [20,68–70]. Lysozyme binds to the n-acetylglucosamine residues and breaks down chitosan. The addition of a crosslinking agent, such as genipin, strengthens the chemical structure of chitosan through covalent bonds and it also may reduce the amount of degradation by lysozyme. The bulky heterocyclical structure of genipin may create a steric hindrance against lysozyme, thus preventing its penetrating and binding to n-acetylglucosamine residues [51]. The lysozyme assay is a basic in vitro test to observe scaffold degradation. There are many other parameters needed to closely mimic the environment of the brain in vitro (pH, temperature, cytokines and chemokines, erosion and inflammatory cells). Ultimately, in vivo tests will be necessary to effectively quantify chitosan microsphere degradation. It is important that the degradation should parallel the ingrowth of new tissue formation. Although genipin did increase the retention of protein within the microsphere, this process was very inefficient. More than half of the protein was lost during the washing steps. Given that the isoelectric point (p*I*) of BSA is 4.7 and its molecular weight is 69.3 kDa, at a pH higher than 4.7 (PBS has a pH of 7.2) BSA will carry a net negative charge, whereas chitosan will carry a net positive charge. This means that there will be ionic interaction between chitosan and BSA, thus slowing down the rate of protein release. FGF-2 is a 17.2 kDa protein with a p*I* of 9.6 and thus carries a net positive charge. This would result in an increased rate of release compared to BSA. Subsequently, the washing steps in an FGF-2 release study would have caused more protein loss than in a BSA release study. Although practical, this method is not economically

efficient, especially when using expensive biologically active peptides like FGF-2; thus we investigated an alternative method to deliver FGF-2.

Heparin has selective binding pockets for growth factors like FGF-2. Heparin binds ionically to chitosan, and genipin can be used for stronger covalent binding. This was verified by FTIR spectrometry and toluidine blue staining. This technique for immobilizing FGF-2 has not been demonstrated using chitosan as the bulk biomaterial. Wissink et al. [71] and Wu et al. [72] both successfully immobilized FGF-2 to heparinized collagen matrices for endothelial cell growth with much success. These scaffolds were crosslinked with the chemical crosslinkers N,N-(3-dimethylaminopropyl)-N′-ethylcarbodiimide and N-hydroxysuccinimide. Shen et al. [73] saw greater 3T3-fibroblast affinity on heparin-modified poly(lactic-co-glycolic acid) scaffolds containing immobilized FGF-2.

The benefit of using genipin-crosslinked chitosan–heparin-FGF-2 complex is that this process does not require stringent washing after attaching the growth factor, unlike the previous technique of encapsulation. Another advantage with this system is that heparin protects the FGF-2 from thermal degradation, thus maintaining its biological activity. Heparin on the substrate also facilitates the binding of FGF-2 to its receptors (FGFR-1, FGFR-3 and FGFR-4) [74]. Furthermore, when FGF-2 is attached to the scaffold it is more readily available to the cells than in standard culture conditions, when it is in solution in the medium. All in all, this functionalized substrate maintains the stem cells in a proliferative state. The preservation of the biological activity of FGF-2 was demonstrated using the neural stem cells in the MTT assay. Zomer Volpato et al. [75] saw similar effects using mesenchymal stem cells on electrospun chitosan nanofiber scaffolds with bound heparin and FGF-2. Genipin crosslinking also allows for a slower degradation of the chitosan microspheres. However, there are still many other factors that may affect their degradation, including, but not limited to, pH, other enzymes and chemicals, macrophages and constant fluid flow. Therefore the degradation rates of both crosslinked and non-crosslinked chitosan microspheres are expected to be faster when transplanted into a cystic lesion.

In this study, we have performed a feasibility test of using immobilized FGF-2 on chitosan–heparin complex membranes for the attachment and survival of neural stem cells. As a control, we have included a standard culture system with soluble FGF-2 ($10\ ng\ ml^{-1}$) since this culture system supports the survival and growth of neural stem cells, as described previously [76]. Although the immobilized FGF-2 culture system provided similar bioactivity for neural stem cells compared to the control condition (a soluble FGF-2 culture system), the immobilized FGF-2 culture system is not directly comparable to the control because the FGF-2 concentrations used for the two culture conditions are different. Further studies are needed to determine the effect of FGF-2 (immobilized vs. soluble) at the same concentration for direct comparison of neural stem cell growth and survival.

Another feature of this design is that cells can be adhered to the surface of the scaffold, which contrasts with the numerous studies that have encapsulated the cells inside spheres or other delivery vehicles [39,77–79]. Encapsulation does not allow for the migration of stem cells from the scaffold into the adjacent tissue, which will be crucial in reconstructing a damaged brain. During embryonic neural development, ventricular zone radial glia extend their processes to the pial surface and their progeny migrate along these radial processes to form the multilaminar neocortex. Future studies will determine whether neural stem cells delivered on this multifunctional scaffold can re-establish a germinal matrix, thus enabling proliferation and migration of neural precursors to promote CNS regeneration after injury.

5. Conclusion

In this study, we have designed and optimized 3-D multifunctional microspheres using natural biopolymers for the delivery of neural stem cells and growth factors into the injured CNS. Heparin was stably crosslinked onto chitosan scaffolds using genipin. The crosslinked chitosan–heparin complex was shown to have a high binding affinity for FGF-2 and good cytocompatibility.

Acknowledgements

This study was partially supported by the New Jersey Commission on Brain Injury Research grant number 08.001.BIR2 awarded to C.D.G. and S.W.L., fellowship grant number CBIR12FEL025 awarded to N.P.S. and the Wallace H. Coulter Foundation.

Appendix A. Figures with essential color discrimination

Certain figures in this article, particularly Figs. 1, and 3–5, are difficult to interpret in black and white. The full color images can be found in the on-line version, at http://dx.doi.org/10.1016/j.actbio.2013.02.043

References

[1] Silver J, Miller JH. Regeneration beyond the glial scar. Nat Rev Neurosci 2004;5:146–56.
[2] Morganti-Kossmann MC, Satgunaseelan L, Bye N, Kossmann T. Modulation of immune response by head injury. Injury 2007;38:1392–400.
[3] Molcanyi M, Riess P, Bentz K, Maegele M, Hescheler J, Schafke B, et al. Trauma-associated inflammatory response impairs embryonic stem cell survival and integration after implantation into injured rat brain. J Neurotrauma 2007;24:625–37.
[4] Harting MT, Sloan LE, Jimenez F, Baumgartner J, Cox Jr CS. Subacute neural stem cell therapy for traumatic brain injury. J Surg Res 2009;153:188–94.
[5] Tate CC, Shear DA, Tate MC, Archer DR, Stein DG, LaPlaca MC. Laminin and fibronectin scaffolds enhance neural stem cell transplantation into the injured brain. J Tissue Eng Regen Med 2009;3:208–17.
[6] Tate MC, Shear DA, Hoffman SW, Stein DG, Archer DR, LaPlaca MC. Fibronectin promotes survival and migration of primary neural stem cells transplanted into the traumatically injured mouse brain. Cell Transplant 2002;11:283–95.
[7] Crompton KE, Goud JD, Bellamkonda RV, Gengenbach TR, Finkelstein DI, Horne MK, et al. Polylysine-functionalised thermoresponsive chitosan hydrogel for neural tissue engineering. Biomaterials 2007;28:441–9.
[8] Mo L, Yang Z, Zhang A, Li X. The repair of the injured adult rat hippocampus with NT-3-chitosan carriers. Biomaterials 2010;31:2184–92.
[9] Lo CM, Wang HB, Dembo M, Wang YL. Cell movement is guided by the rigidity of the substrate. Biophys J 2000;79:144–52.
[10] Wang HB, Dembo M, Wang YL. Substrate flexibility regulates growth and apoptosis of normal but not transformed cells. Am J Physiol Cell Physiol 2000;279:C1345–50.
[11] Engler AJ, Sen S, Sweeney HL, Discher DE. Matrix elasticity directs stem cell lineage specification. Cell 2006;126:677–89.
[12] Balgude AP, Yu X, Szymanski A, Bellamkonda RV. Agarose gel stiffness determines rate of DRG neurite extension in 3D cultures. Biomaterials 2001;22:1077–84.
[13] Willits RK, Skornia SL. Effect of collagen gel stiffness on neurite extension. J Biomater Sci Polym Ed 2004;15:1521–31.
[14] Philip Lamoreux REBaSRH. Direct evidence that growth cones pull. Nature 1989;340:159–62.
[15] Kai D, Prabhakaran MP, Stahl B, Eblenkamp M, Wintermantel E, Ramakrishna S. Mechanical properties and in vitro behavior of nanofiber–hydrogel composites for tissue engineering applications. Nanotechnology 2012;23:095705.
[16] Barbucci R. Hydrogels: Biological Properties and Applications. 2009;XII:200.
[17] Sinha VR, Singla AK, Wadhawan S, Kaushik R, Kumria R, Bansal K, et al. Chitosan microspheres as a potential carrier for drugs. Int J Pharm 2004;274:1–33.
[18] Kou JH, Emmett C, Shen P, Aswani S, Iwamoto T, Vaghefi F, et al. Bioerosion and biocompatibility of poly(d,l-lactic-co-glycolic acid) implants in brain. J Controlled Release 1997;43:123–30.
[19] Seo MC, Kim S, Kim SH, Zheng LT, Park EK, Lee WH, et al. Discoidin domain receptor 1 mediates collagen-induced inflammatory activation of microglia in culture. J Neurosci Res 2008;86:1087–95.
[20] Freier T, Koh HS, Kazazian K, Shoichet MS. Controlling cell adhesion and degradation of chitosan films by N-acetylation. Biomaterials 2005;26:5872–8.
[21] Khor E, Lim LY. Implantable applications of chitin and chitosan. Biomaterials 2003;24:2339–49.

[22] Jumaa M, Furkert FH, Muller BW. A new lipid emulsion formulation with high antimicrobial efficacy using chitosan. Eur J Pharm Biopharm 2002;53:115–23.
[23] Bhattarai N, Gunn J, Zhang M. Chitosan-based hydrogels for controlled, localized drug delivery. Adv Drug Deliv Rev 2010;62:83–99.
[24] Francesko A, Tzanov T. Chitin, chitosan and derivatives for wound healing and tissue engineering. Adv Biochem Eng Biotechnol 2011;125:1–27.
[25] Cho CH, Eliason JF, Matthew HW. Application of porous glycosaminoglycan-based scaffolds for expansion of human cord blood stem cells in perfusion culture. J Biomed Mater Res A 2008;86:98–107.
[26] Kim HJ, Lee JH, Kim SH. Therapeutic effects of human mesenchymal stem cells on traumatic brain injury in rats: secretion of neurotrophic factors and inhibition of apoptosis. J Neurotrauma 2010;27:131–8.
[27] Madihally SV, Matthew HW. Porous chitosan scaffolds for tissue engineering. Biomaterials 1999;20:1133–42.
[28] Hussain A, Collins G, Yip D, Cho CH. Functional 3-D cardiac co-culture model using bioactive chitosan nanofiber scaffolds. Biotechnol Bioeng 2013;110:637–47.
[29] Shi W, Nie D, Jin G, Chen W, Xia L, Wu X, et al. BDNF blended chitosan scaffolds for human umbilical cord MSC transplants in traumatic brain injury therapy. Biomaterials 2012;33:3119–26.
[30] Eroglu H, Nemutlu E, Turkoglu OF, Nacar O, Bodur E, Sargon MF, et al. A quadruped study on chitosan microspheres containing atorvastatin calcium: preparation, characterization, quantification and in-vivo application. Chem Pharm Bull (Tokyo) 2010;58:1161–7.
[31] Cho Y, Shi R, Borgens RB. Chitosan produces potent neuroprotection and physiological recovery following traumatic spinal cord injury. J Exp Biol 2010;213:1513–20.
[32] Nomura H, Zahir T, Kim H, Katayama Y, Kulbatski I, Morshead CM, et al. Extramedullary chitosan channels promote survival of transplanted neural stem and progenitor cells and create a tissue bridge after complete spinal cord transection. Tissue Eng Part A 2008;4:649–65.
[33] Crompton KE, Tomas D, Finkelstein DI, Marr M, Forsythe JS, Horne MK. Inflammatory response on injection of chitosan/GP to the brain. J Mater Sci Mater Med 2006;17:633–9.
[34] Turkoglu OF, Eroglu H, Gurcan O, Bodur E, Sargon MF, Oner L, et al. Local administration of chitosan microspheres after traumatic brain injury in rats: a new challenge for cyclosporine – a delivery. Br J Neurosurg 2010;24:578–83.
[35] Turkoglu OF, Eroglu H, Okutan O, Burul E, Sargon MF, Ozer N, et al. The efficiency of dexamethasone sodium phosphate-encapsulated chitosan microspheres after cold injury. Surg Neurol 2005;64(Suppl 2):S11–6.
[36] Chandy T, Das GS, Rao GH. 5-Fluorouracil-loaded chitosan coated polylactic acid microspheres as biodegradable drug carriers for cerebral tumours. J Microencapsul 2000;17:625–38.
[37] Hassan EE, Gallo JM. Targeting anticancer drugs to the brain. I: Enhanced brain delivery of oxantrazole following administration in magnetic cationic microspheres. J Drug Target 1993;1:7–14.
[38] Kim S, Gaber MW, Zawaski JA, Zhang F, Richardson M, Zhang XA, et al. The inhibition of glioma growth in vitro and in vivo by a chitosan/ellagic acid composite biomaterial. Biomaterials 2009;30:4743–51.
[39] Maysinger D, Berezovskaya O, Fedoroff S. The hematopoietic cytokine colony stimulating factor 1 is also a growth factor in the CNS: (II). Microencapsulated CSF-1 and LM-10 cells as delivery systems. Exp Neurol 1996;141:47–56.
[40] Guo X, Zahir T, Mothe A, Shoichet MS, Morshead CM, Katayama Y, et al. The effect of growth factors and soluble Nogo-66 receptor protein on transplanted neural stem/progenitor survival and axonal regeneration after complete transection of rat spinal cord. Cell Transplant 2012;21:1177–97.
[41] Ribatti D, Roncali L, Nico B, Bertossi M. Effects of exogenous heparin on the vasculogenesis of the chorioallantoic membrane. Acta Anat (Basel) 1987;130:257–63.
[42] Folkman J, Taylor S, Spillberg C. The role of heparin in angiogenesis. Ciba Found Symp 1983;100:132–49.
[43] Vasavada VA, Praveen MR, Shah SK, Trivedi RH, Vasavada AR. Anti-inflammatory effect of low-molecular-weight heparin in pediatric cataract surgery: a randomized clinical trial. Am J Ophthalmol 2012;154(252–8):e4.
[44] Cervera A, Justicia C, Reverter JC, Planas AM, Chamorro A. Steady plasma concentration of unfractionated heparin reduces infarct volume and prevents inflammatory damage after transient focal cerebral ischemia in the rat. J Neurosci Res 2004;77:565–72.
[45] Ashikari-Hada S, Habuchi H, Kariya Y, Itoh N, Reddi AH, Kimata K. Characterization of growth factor-binding structures in heparin/heparan sulfate using an octasaccharide library. J Biol Chem 2004;279:12346–54.
[46] Sommer A, Rifkin DB. Interaction of heparin with human basic fibroblast growth factor: protection of the angiogenic protein from proteolytic degradation by a glycosaminoglycan. J Cell Physiol 1989;138:215–20.
[47] Sun D, Bullock MR, McGinn MJ, Zhou Z, Altememi N, Hagood S, et al. Basic fibroblast growth factor-enhanced neurogenesis contributes to cognitive recovery in rats following traumatic brain injury. Exp Neurol 2009;216:56–65.
[48] Yoshimura S, Teramoto T, Whalen MJ, Irizarry MC, Takagi Y, Qiu J, et al. FGF-2 regulates neurogenesis and degeneration in the dentate gyrus after traumatic brain injury in mice. J Clin Invest 2003;112:1202–10.
[49] Vergano-Vera E, Mendez-Gomez HR, Hurtado-Chong A, Cigudosa JC, Vicario-Abejon C. Fibroblast growth factor-2 increases the expression of neurogenic genes and promotes the migration and differentiation of neurons derived from transplanted neural stem/progenitor cells. Neuroscience 2009;162:39–54.
[50] Stachowiak EK, Maher PA, Tucholski J, Mordechai E, Joy A, Moffett J, et al. Nuclear accumulation of fibroblast growth factor receptors in human glial cells – association with cell proliferation. Oncogene 1997;14:2201–11.
[51] Mi FL, Tan YC, Liang HF, Sung HW. In vivo biocompatibility and degradability of a novel injectable-chitosan-based implant. Biomaterials 2002;23:181–91.
[52] Sung HW, Huang RN, Huang LL, Tsai CC. In vitro evaluation of cytotoxicity of a naturally occurring cross-linking reagent for biological tissue fixation. J Biomater Sci Polym Ed 1999;10:63–78.
[53] Harris R, Lecumberri E, Heras A. Chitosan–genipin microspheres for the controlled release of drugs: clarithromycin, tramadol and heparin. Mar Drugs 2010;8:1750–62.
[54] Yamazaki M, Chiba K, Mohri T, Hatanaka H. Cyclic GMP-dependent neurite outgrowth by genipin and nerve growth factor in PC12h cells. Eur J Pharmacol 2004;488:35–43.
[55] Koo HJ, Lim KH, Jung HJ, Park EH. Anti-inflammatory evaluation of gardenia extract, geniposide and genipin. J Ethnopharmacol 2006;103:496–500.
[56] Nam KN, Choi YS, Jung HJ, Park GH, Park JM, Moon SK, et al. Genipin inhibits the inflammatory response of rat brain microglial cells. Int Immunopharmacol 2010;10:493–9.
[57] Thakur G, Mitra A, Rousseau D, Basak A, Sarkar S, Pal K. Crosslinking of gelatin-based drug carriers by genipin induces changes in drug kinetic profiles in vitro. J Mater Sci Mater Med 2011;22:115–23.
[58] Koriyama Y, Takagi Y, Chiba K, Yamazaki M, Arai K, Matsukawa T, et al. Neuritogenic activity of a genipin derivative in retinal ganglion cells is mediated by retinoic acid receptor beta expression through nitric oxide/S-nitrosylation signaling. J Neurochem 2011;119:1232–42.
[59] Yuan Y. The effect of cross-linking of chitosan microspheres with genipin on protein release. Carbohydr Polym 2007;68:561–7.
[60] Mosmann T. Rapid colorimetric assay for cellular growth and survival: application to proliferation and cytotoxicity assays. J Immunol Methods 1983;65:55–63.
[61] Zeng Y, Liu YS. Vascular endothelial cells and pituitary hormone producing cells derived from embryonic stem cells therapy for hypopituitarism. Med Hypotheses 2011;77:680–1.
[62] Solorio L, Zwolinski C, Lund AW, Farrell MJ, Stegemann JP. Gelatin microspheres crosslinked with genipin for local delivery of growth factors. J Tissue Eng Regen Med 2010;4:514–23.
[63] Guo XL, Yang KS, Hyun JY, Kim WS, Lee DH, Min KE, et al. Morphology and metabolism of Ba-alginate-encapsulated hepatocytes with galactosylated chitosan and poly(vinyl alcohol) as extracellular matrices. J Biomater Sci Polym Ed 2003;14:551–65.
[64] Kim SE, Park JH, Cho YW, Chung H, Jeong SY, Lee EB, et al. Porous chitosan scaffold containing microspheres loaded with transforming growth factor-beta1: implications for cartilage tissue engineering. J Control Release 2003;91:365–74.
[65] Tolaimate A, Desbrie'res J, Rhazi M, Alagui A, Vincendron M, Vottero P. On the influence of deacetylation process on the physicochemical characteristics of chitosan from squid chitin. Polymer 2000;41:2463–9.
[66] Lee KY, Ha WS, Park WH. Blood compatibility and biodegradability of partially N-acylated chitosan derivatives. Biomaterials 1995;16:1211–6.
[67] Onishi H, Machida Y. Biodegradation and distribution of water-soluble chitosan in mice. Biomaterials 1999;20:175–82.
[68] Peluso G, Petillo O, Ranieri M, Santin M, Ambrosio L, Calabro D, et al. Chitosan-mediated stimulation of macrophage function. Biomaterials 1994;15:1215–20.
[69] Barbosa JN, Amaral IF, Aguas AP, Barbosa MA. Evaluation of the effect of the degree of acetylation on the inflammatory response to 3D porous chitosan scaffolds. J Biomed Mater Res A 2010;93:20–8.
[70] Hidaka Y, Ito M, Mori K, Yagasaki H, Kafrawy AH. Histopathological and immunohistochemical studies of membranes of deacetylated chitin derivatives implanted over rat calvaria. J Biomed Mater Res 1999;46:418–23.
[71] Wissink MJ, Beernink R, Pieper JS, Poot AA, Engbers GH, Beugeling T, et al. Binding and release of basic fibroblast growth factor from heparinized collagen matrices. Biomaterials 2001;22:2291–9.
[72] Wu JM, Xu YY, Li ZH, Yuan XY, Wang PF, Zhang XZ, et al. Heparin-functionalized collagen matrices with controlled release of basic fibroblast growth factor. J Mater Sci Mater Med 2011;22:107–14.
[73] Shen H, Hu X, Yang F, Bei J, Wang S. Cell affinity for bFGF immobilized heparin-containing poly(lactide-co-glycolide) scaffolds. Biomaterials 2011;32:3404–12.
[74] Bottcher RT, Niehrs C. Fibroblast growth factor signaling during early vertebrate development. Endocr Rev 2005;26:63–77.
[75] Zomer Volpato F, Almodovar J, Erickson K, Popat KC, Migliaresi C, Kipper MJ. Preservation of FGF-2 bioactivity using heparin-based nanoparticles, and their delivery from electrospun chitosan fibers. Acta Biomater 2012;8:1551–9.
[76] Li H, Babiarz J, Woodbury J, Kane-Goldsmith N, Grumet M. Spatiotemporal heterogeneity of CNS radial glial cells and their transition to restricted precursors. Dev Biol 2004;271:225–38.
[77] Zielinski BA, Aebischer P. Chitosan as a matrix for mammalian cell encapsulation. Biomaterials 1994;15:1049–56.
[78] Leipzig ND, Wylie RG, Kim H, Shoichet MS. Differentiation of neural stem cells in three-dimensional growth factor-immobilized chitosan hydrogel scaffolds. Biomaterials 2011;32:57–64.
[79] Nicodemus GD, Bryant SJ. Cell encapsulation in biodegradable hydrogels for tissue engineering applications. Tissue Eng Part B Rev 2008;14:149–65.